ACS OMEGA

http://pubs.acs.org/journal/acsodf

Article

The Effectiveness of Pahae Natural Zeolite−Cocoa Shell Activated Charcoal Nanofilter as a Water Adsorber in Bioethanol Purification

Susilawati,* Yuan Alfinsyah Sihombing, Siti Utari Rahayu, Lilik Waldiansyah, and Yuni Yati Br Sembiring

Cite This: *ACS Omega* 2022, 7, 38417−38425

Read Online

ACCESS | Metrics & More | Article Recommendations

ABSTRACT: Pahae natural zeolite potentially can be used as a filtration material because of its high adsorption capacity. However, it is known that other supportive materials such as activated charcoal are needed to optimize the utilization of natural zeolite as an adsorber. This study aims to investigate the potential use of activated charcoal which was synthesized from cocoa shells waste and natural zeolite in nanosize as the adsorber in order to increase the concentration of bioethanol. The mixing process of nanozeolite and activated charcoal of cocoa shells was carried out through mechanical mixing, while the nanofilter was made using a press-printing technique followed by sintering at several temperature variations. The results showed that the activated zeolite produced in this study has a particle size of 118.4 nm with water absorption capacity of 52.08%. In line with that, the bioethanol concentration was increased up to 78.92% during the adsorption with a 45 min contact time with water vapor. Thus, based on the results, it can be concluded that nanosized zeolite-based adsorbents and activated charcoal produced from cocoa shells can be utilized as adsorbers to significantly increase the concentration of bioethanol generated.

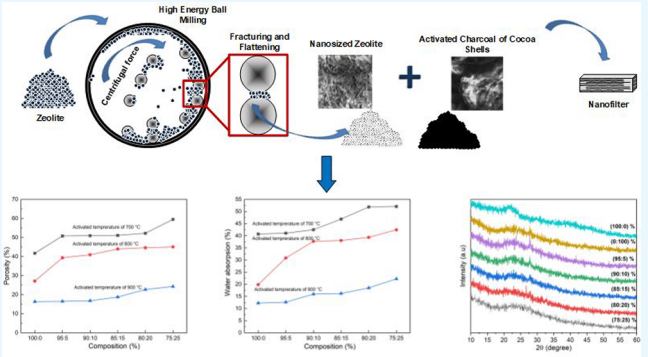

1. INTRODUCTION

The lower fossil energy deposits become the basis for the development of research to find other energy sources in the form of renewable energy that is environmentally friendly and sustainable.[1] With current usage patterns, it is estimated that the remaining fossil energy will be depleted within the next 40−50 years.[2]

Biofuel is one of the renewable energy sources with abundant natural material sources. Bioethanol is a type of biofuel that is currently being researched. Bioethanol can be produced from natural carbohydrates such as sugar cane, potatoes, cassava, and corn.[3] Bioethanol production is expected to rise as a result of its utility as a gasoline additive. It is well-known that adding bioethanol to gasoline raises the octane number of the gasoline. It is difficult to manufacture bioethanol with high purity. Meanwhile, ethanol with a purity level of >99.5% is required for use as a fuel, and it must be completely dry and anhydrous to be noncorrosive.[4] Distillation and adsorption are two techniques that can be used to increase the purity of bioethanol. The distillation process is known for producing high-purity ethanol in a relatively short time, but it requires a large amount of raw material because reagents and catalysts must be continuously flowed during the process.[5,6] Meanwhile, other technologies, such as adsorption, are being promoted in the ethanol purification process because it requires little energy while producing a high level of productivity and purity. Adsorption is a purification technique that separates materials from an unwanted gas or liquid mixture.[7,8] The material to be separated is attracted by the solid adsorbent surface and bound by the surface forces. As a result, the type of adsorbent chosen has a significant impact on the success of this process. Adsorbents of high quality usually have a large adsorption surface area. Zeolite is one of the adsorbents that is commonly used to separate ethanol−water mixtures.[9,10]

Zeolite is an inorganic mineral rock that is widely used in Indonesia. Zeolite is a porous material with excellent physicochemical properties such as high cation exchange capacity, cation selectivity, and large pore volume.[11] Zeolite is used as an adsorber because of its regular amorphous structure with interconnected cavities in all directions, the ability to absorb small molecules, and a very large surface area.[12,13] Moreover, the ability of zeolites to exchange catalysts via cation adsorption is what makes them beneficial to be used as adsorber materials.[14,15] In addition, zeolite is also known as a porous material and has several practical uses, such as filters

Received: June 9, 2022
Accepted: October 7, 2022
Published: October 19, 2022

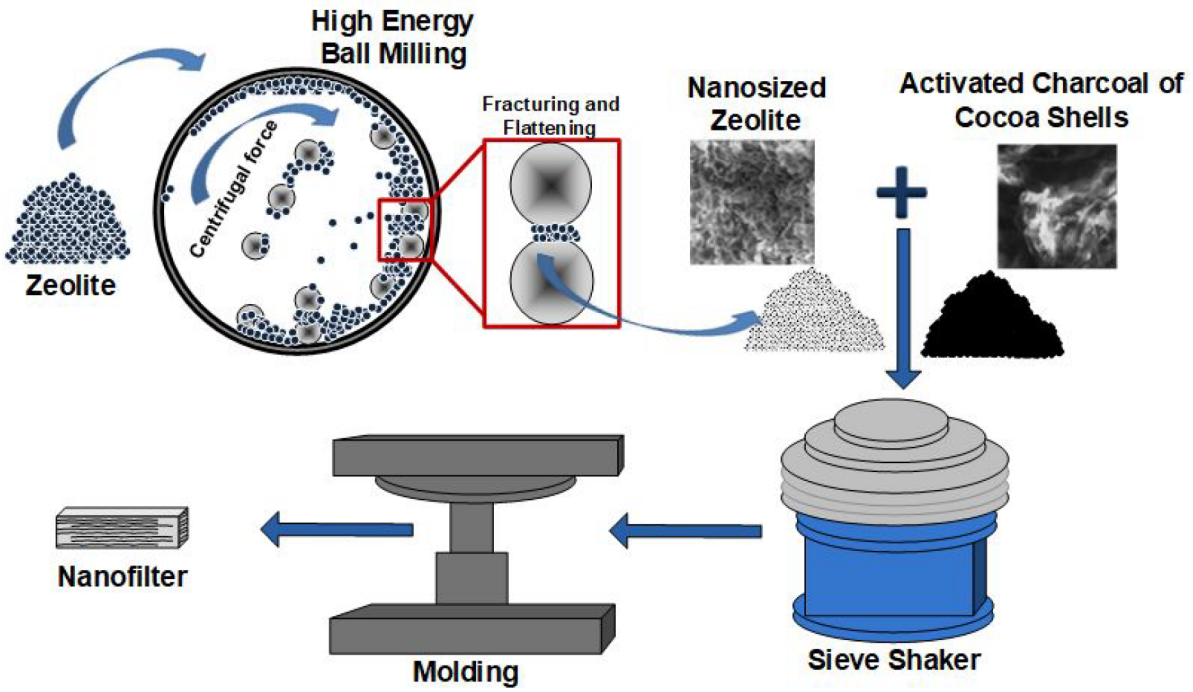

Figure 1. Illustration of nanofilter fabrication (Microsoft Visio 2007 was used by the author to create the illustration).

and absorbents of moisture.[16−18] The effect of zeolite adsorption is affected by the number and size of open pores on the zeolite surface.[19] As a result, the activation process has a significant impact in determining the effectiveness of the zeolite capacity.[20,21]

Pahae-activated natural zeolite can absorb up to 53.82% of its weight in water. A previous study found that Pahae natural zeolite with a mesh size of 200 had a higher water vapor adsorption capacity than Cikalong natural zeolite. Due to the high adsorption capacity of Pahae natural zeolite, this porous material has the potential to be used as an adsorbent.[16] Furthermore, another study reported the use of nanosized Pahae natural zeolite, which is known to be able to adsorb water up to 73.81%, in bioethanol purification via distillation and adsorption techniques and succeeded in increasing the concentration of bioethanol to 88.97% with a contact time of 45 min.[22,23] In addition, the size of the zeolite plays an important role in the rate of water vapor absorption:[16−18] the smaller the particle size of the zeolite the greater the surface area available for adsorption, and this affects the rate of adsorption of the material.[24,25] While activated carbon is used in this study because it is the most commonly used adsorber and has been successfully used in industrial wastewater and gas treatment for environmental protection and material recovery objectives, particularly in the purification of biofuel,[26] these qualities are due to its inherent characteristics, which include a large surface area, a microporous structure, a high porosity, and a high adsorption capacity.[27,28]

Nanofilters are solid-structured materials with repeated dimensions in the nanometer range, consisting of a combination of two or more inorganic/organic molecules containing at least one molecule of nanoscale size consisting of several materials that can share the role of a matrix or filler.[29,30] The nanofilter in this study was made of zeolite material, which serves as a matrix, and activated charcoal from cocoa rind, which serves as a filler. Cocoa shells were chosen because they are hydrophobic and have a high charcoal content, so they has the potential to be used as a source of activated charcoal.[31] In addition, this research is useful to increase the value of cocoa shell waste with low and economical processing costs. Furthermore, the basis of this research is supported by previous reports of the potential utilization of activated charcoal from cocoa shells combined with clay as an adsorber.[32,33] In line with that, other studies have also reported the potential use of a mixture of zeolite with cocoa rind as a filler.[17] The aim of this research is to create a zeolite−activated charcoal nanofilter from cocoa shells and test its efficacy for bioethanol purification. To investigate the characteristics of the zeolite-activated charcoal nanofilter obtained from cocoa shells, several characterizations were performed, including porosity, water absorption, hardness, SEM, EDX, XRD, PSA, FT-IR, gas chromatography, and XRF.

2. MATERIALS AND METHODS

2.1. Materials. Pahae natural zeolite was obtained from Pahae District (North Sumatra, Indonesia). Cocoa peel was obtained from Gunung Village, Tiga Binanga District (North Sumatra, Indonesia). 96% sulfuric acid was purchased from Mallinckrodt Baker, (Paris, KY). Bioethanol with a concentration of 96% was purchased from Merck (Darmstadt, Germany).

2.2. Pahae Natural Zeolite Nanoparticles Activation and Preparation. Pahae natural zeolite powder that passed a 74 m (200 mesh) filter was chemically activated with 6% sulfuric acid and agitated for 4 h at 70 °C at 550 rpm. After 4 h, Pahae natural zeolite was cleaned with distilled water until the pH was neutral and then dried in a 100 °C oven for 1 h. The high energy milling (HEM E3D) process was then used to create Pahae natural zeolite nanoparticles. Into the HEM E3D jar, 11 ball milling with a weight of 3.52 g per ball was used to process every 4.84 g of Pahae natural zeolite.[22,31]

https://doi.org/10.1021/acsomega.2c03614
ACS Omega 2022, 7, 38417−38425

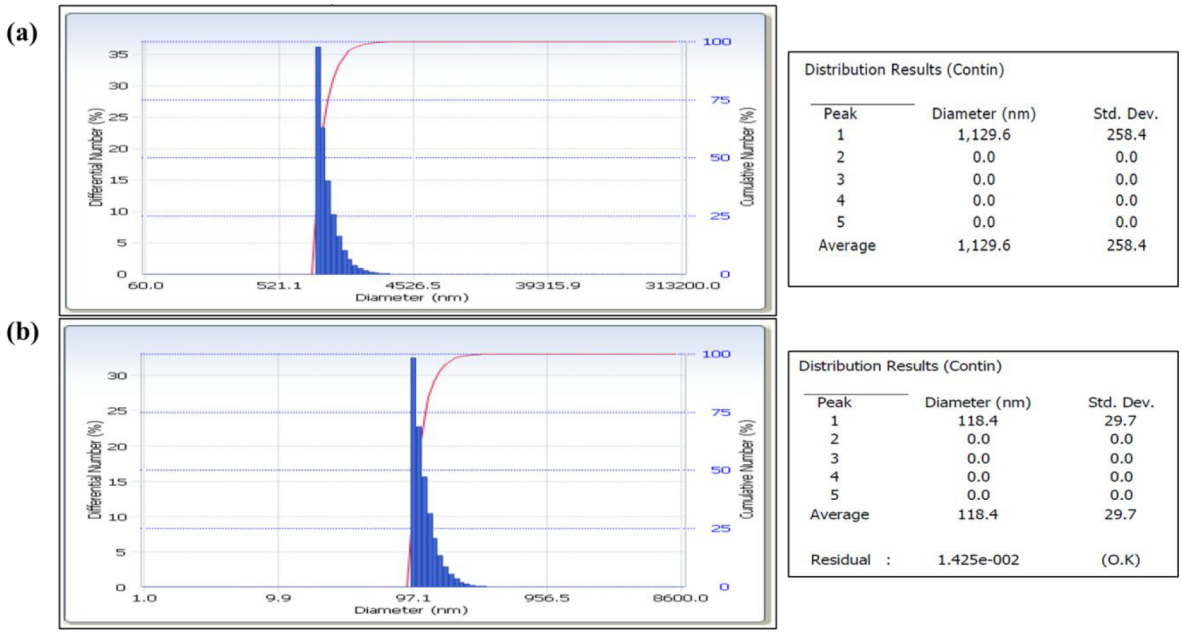

Figure 2. PSA results of activated zeolite (a) before and (b) after the ball-milling process.

2.3. Cocoa Shells Charcoal Process. The cocoa skin that was used had a yellow color. Then the cocoa skin was cleaned from any attached impurities, such as seeds and fruit flesh. After that, the cocoa shells were cut into small pieces and then dried under sunlight until dry (moisture content <8%). Then charcoal was made by carbonization using an MEMMERT UN55 oven (Germany) at 1500 °C for 1 h. After becoming charcoal, the cocoa shells were crushed using a mortar. The crushed cocoa shells were then sieved using a 74 m (200 mesh) sieve.

2.4. Zeolite-Activated Charcoal Nanofilter Cocoa Shells Production. Mixing and sintering processes were used in this study to create zeolite nanofilters and cocoa shell activated charcoal. These two ingredients were combined and placed in a 550 cc YM1832 Yami shaker. This mixture was then stirred for 5 min with variations in composition, namely (100:0)%, (95:5)%, (90:10)%, (85:15)%, (80:20)%, and (75:25)% wt. A few drops of aquadest were added to the mixture, which was then stirred several times. The sample was then placed for 10 min in a hydraulic press Ytd27-200t with a mass of 5 tons. For the other mixing compositions, the same molding procedure was used. After that, the sample was left out in the open for a week to avoid cracking during the heating process. After a week, the samples were physically activated for 4 h at temperatures of 700, 800, and 900 °C. All of the steps involved in making the nanofilter are illustrated in Figure 1.

2.5. Characterizations. The particle size distribution of the samples was determined using a Malvern Mastersizer 2000 laser light-scattering particle size analyzer, and the base of the spherical equivalent diameter of 300 individual particles of each sample was estimated. The water absorption capacity of the material is evaluated according to ASTM C20-00[34] and can be calculated according to eq 1. The porosity of the material was evaluated by referring to ASTM C642-06[35] and calculated using eq 2. The hardness test was conducted using a Matsuzawa Seiki Hardness Tester (Japan) with a load mass of 1 kg and a holding period of 30 s. The hardness value is then calculated using eq 3.

$$\%\text{water absorption} = \left(\frac{\text{final mass} - \text{initial mass}}{\text{initial mass}}\right) \times 100 \quad (2)$$

$$\%\text{porosity} = \left(\frac{\text{final mass} - \text{initial mass}}{\text{density of water} \times \text{water volume}}\right) \times 100 \quad (1)$$

$$H_v = 1,8544\frac{F}{d^2} \quad (3)$$

A scanning electron microscope (SEM) model JEOL JSM6390, in conjunction with an energy-dispersive X-ray (EDX) analyzer from Oxford Instruments, was used to examine the morphology and elemental composition of initial materials, intermediates, and end products. The crystallinity phase of the obtained sample was investigated using a Philips PW 1050 X-ray diffractometer. 2θ of the samples was scanned from 7 to 70°. The FTIR spectra of the samples were analyzed using the PerkinElmer System IR 2000 spectrometer at a wavenumber of 1400−400 cm^{-1}, with 100 scans using KBr pellets technic. Using an XGT-5200 XRF spectrometer, the chemical composition of the sample was determined. The ratio $[SiO_2]/[Al_2O_3]$ was calculated using this information.

2.6. Gas Chromatography Test for Bioethanol Purification. 100 mL of 40% bioethanol was poured into a glass beaker which already contained 50 g of nanofilter while stirring at 550 rpm with various contact times of 30, 45, 60, 75, and 90 min. The bioethanol was then evaporated using a rotary evaporator with a rotating speed of 110−120 rpm at a temperature of 78 °C. Evaporated bioethanol was then analyzed using gas chromatography. The concentration obtained was then compared with 96% ethanol.[36,37]

3. RESULTS AND DISCUSSION

3.1. Particle Size Analyzer (PSA) Test. The PSA analysis was conducted to determine the sample pore diameter of 74 m (200 mesh) zeolite particles before and after ball milling with HEM. The results of the analysis are shown in Figure 7.

https://doi.org/10.1021/acsomega.2c03614
ACS Omega 2022, 7, 38417−38425

The average diameter of the activated Pahae natural zeolite was determined using PSA in Figure 2a,b. The PSA test findings in Figure 2a demonstrate that the activated zeolite measuring 74 m (200 mesh) before being processed with ball milling has a diameter distribution of about 1129.6 nm, while the PSA test findings in Figure 2b demonstrate that the activated zeolite measuring 74 m (200 mesh) after being processed with ball milling has a sample diameter distribution of roughly 118.4 nm. This demonstrates that decreasing the size of the zeolite using ball milling equipment combined with HEM treatment is successful. During physical treatment, HEM treatment is vital, and 10 h of milling contact time can increase the efficacy of particle collisions, resulting in nanosized particles.[38] The top-down method using HEM can cause agglomeration if the process is carried out excessively.[39]

3.2. Water Absorption Test. The water absorption test of the nanofilters was carried out by referring to ASTM C20-00, and the results are shown in Figure 3. According to the test

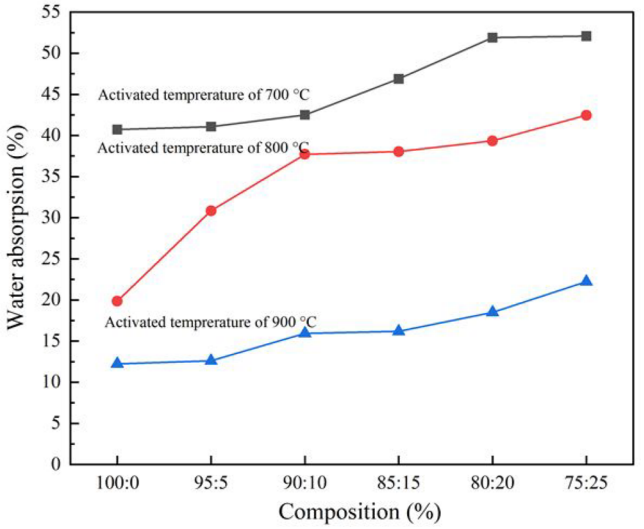

Figure 3. Correlation graph of composition againts water absorbsion.

results, the sample with a nanofilter composition of (75:25)% which is activated at 700 °C has the highest water absorption value with a value of 52.08%. Meanwhile, the lowest water absorption value is shown in the (100:0)% composition at 900 °C, which is only able to absorb water by 12.24%. Based on the tests carried out, it was analyzed that the addition of activated charcoal filler of cocoa shell on the nanofilter was able to increase the value of water absorption. Activated charcoal has a large surface area of up to 1500 m^2/g and an abundance of functional groups on its surface. As a result, it has been extensively employed for gas separation, solvent recovery, wastewater treatment, and as an effective catalyst in the process of biodiesel production.[40] From the results, it can also be analyzed that the water absorption value produced is directly proportional to the porosity value, where the larger the pores or cavities of a zeolite the higher the water absorption value. This is also in line with the results of the porosity test where in the water absorption test it was found that an increase in temperature in the activation process resulted in a decrease in water absorption in the nanofilter, where the higher the temperature, the smaller the water absorption value. This can occur because the surface of the nanofilter is closed; as a result, the distribution of pores is getting smaller and thus inhibits the water absorption process.

3.3. Porosity Test. Porosity testing aims to determine the effect of different combustion temperatures on the size of the pore diameter on the surface of the nanofilter. Calculation of nanofilter porosity is determined by subtracting the dry mass of the wet mass of the nanofilter compared to the density and volume of water. The results obtained are shown in Figure 4.

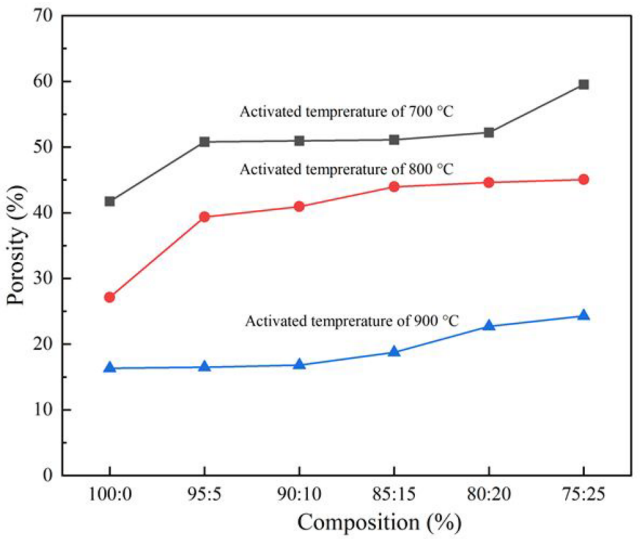

Figure 4. Correlation graph of composition against porosity.

According to the results shown in Figure 4, the sample with a nanofilter composition of (75:25) % that was activated at 700 °C had the highest porosity value of 59.52% when compared to the other samples. The physicochemical features of these materials may be preserved by exposing them to a temperature of 700 °C, producing porous structures, and increasing the reactivity of this material, resulting in zeolite-Activated carbon with great thermal stability.[41−43] Physical activation mainly refers to dry oxidation, which involves the reaction of the samples with gaseous (CO_2 and air), steam, or a combination of gaseous and steam at a temperature of 700 °C when the carbon dioxide was chosen during activation.[44,45] Meanwhile, samples with a (100:0) % nanofilter composition that were activated at 900 °C had the lowest porosity value of 16.34%. This suggests that adding cocoa shell activated charcoal filler to the nanofilter can increase the porosity value of the produced nanofilter. However, too high a temperature during the activation process is known to cause a decrease in the porosity of the sample. This could be experienced by the samples due to high-temperature activation, which causes a decrease in the distribution of pores on the adsorber as well as pore closure, which reduces pore diameter.

3.4. Hardness Test. The Hardness Vickers Tokyo tool was used to conduct a hardness test on a zeolite-activated charcoal nanofilter of cocoa shells. The results are shown in Figure 5. The depicted data were obtained from tests on several samples of nanofilters with varying compositions of zeolite and activated charcoal of cocoa shells. In the figure, it can be seen that the highest hardness value was observed in the sample with a (100:0)% nanofilter composition which was activated at a temperature of 900 °C with a hardness value of 601.970 MPa. Meanwhile, the lowest hardness value of

https://doi.org/10.1021/acsomega.2c03614
ACS Omega 2022, 7, 38417−38425

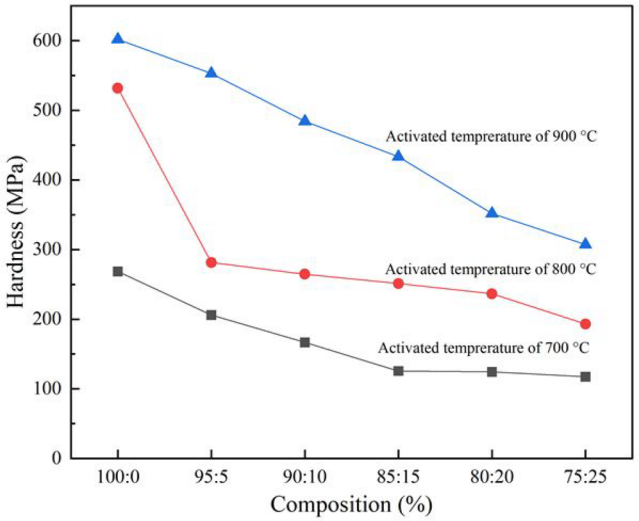

Figure 5. Correlation graph of composition againts hardness.

117.410 MPa was obtained in a sample with a composition of (75:25)% that was activated at a temperature of 700 °C. According to the results, the increase in activation temperature is correlated to the increase in sample hardness. This can be attributed to the high temperature used in the activation process, which reduces and tightens the pore diameter of the nanofilter, thereby increasing its hardness.

The hardness test results indicate that the hardness test is inversely proportional to the physical properties test. The addition of cocoa shell activated charcoal filler to the nanofilter is known to be unable to increase the hardness value. The hardness values of the activated samples at temperatures of 700, 800, and 900 °C continued to decrease when the mass of activated charcoal powder from cocoa shells continued to increase. This is due to the fact that the process of making samples using traditional printing and pressing techniques results in uneven distribution of zeolite and activated charcoal from cocoa shells. Furthermore, indications of the presence of vacancies between particles, which cause trapped oxygen in the sample during the compaction process, as well as the presence of impurities which prevent good intersurface bonding between nanofilter constituents, are thought to be factors that can reduce the hardness of the nanofilter.

3.5. Morphological Analysis. A scanning electron microscope (SEM) was used to analyze the surface morphology of the sample and determine the size of the pore diameter.

The results of morphological evaluations on all variations of the composition of the nanofilter activated at 700 °C are shown in Figure 6. The sample in this variation was chosen for SEM testing because it exhibited the optimum porosity and water absorption value compared to samples on others activation temperatures. The morphological test results on the five composition variations, which were activated at a temperature of 700 °C, revealed that the material composition

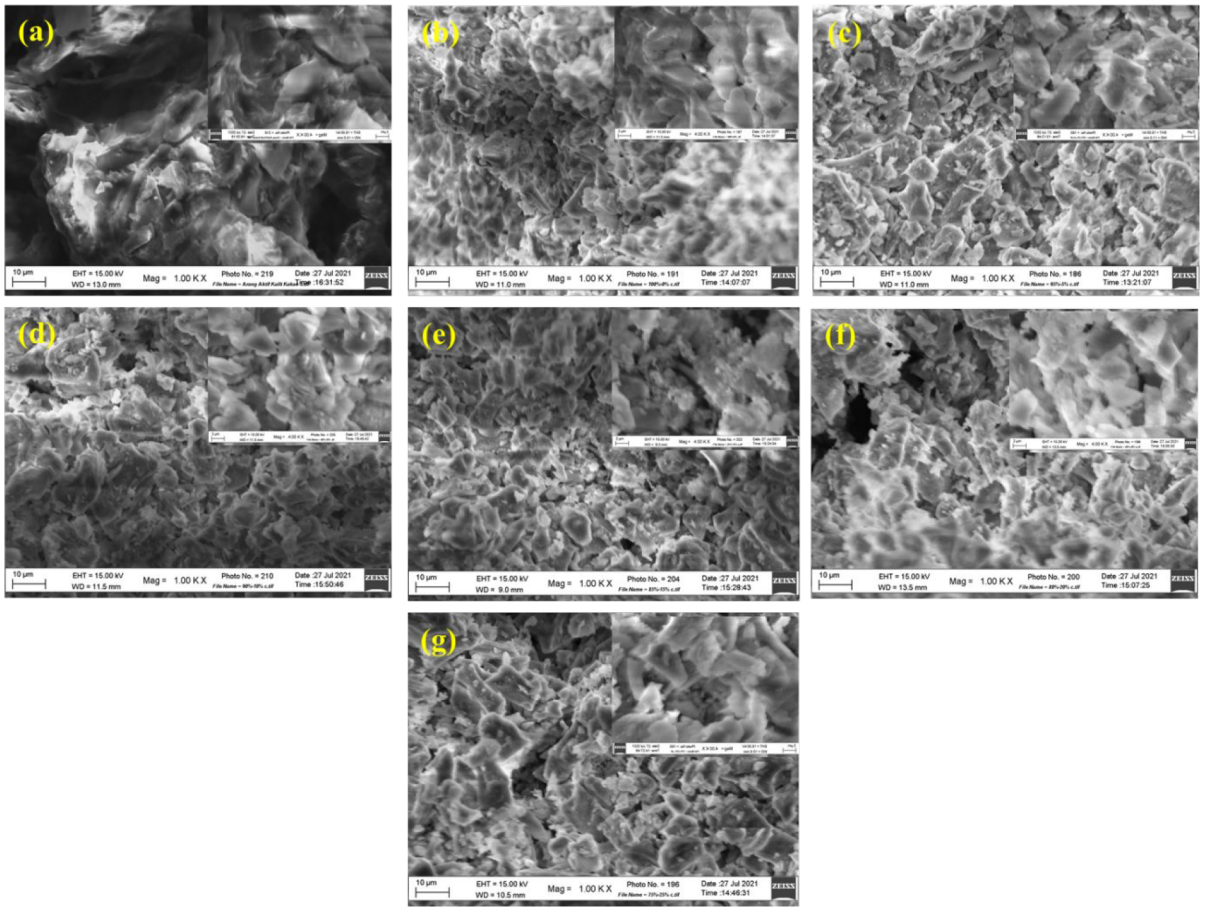

Figure 6. Surface morphology of the sample: (a) (0:100)%; (b) (100:0)%; (c) (95:5)%; (d) (90:10)%; (e) (85:15)%; (f) (80:20)%; and (g) (75:25)%.

https://doi.org/10.1021/acsomega.2c03614
ACS Omega 2022, 7, 38417−38425

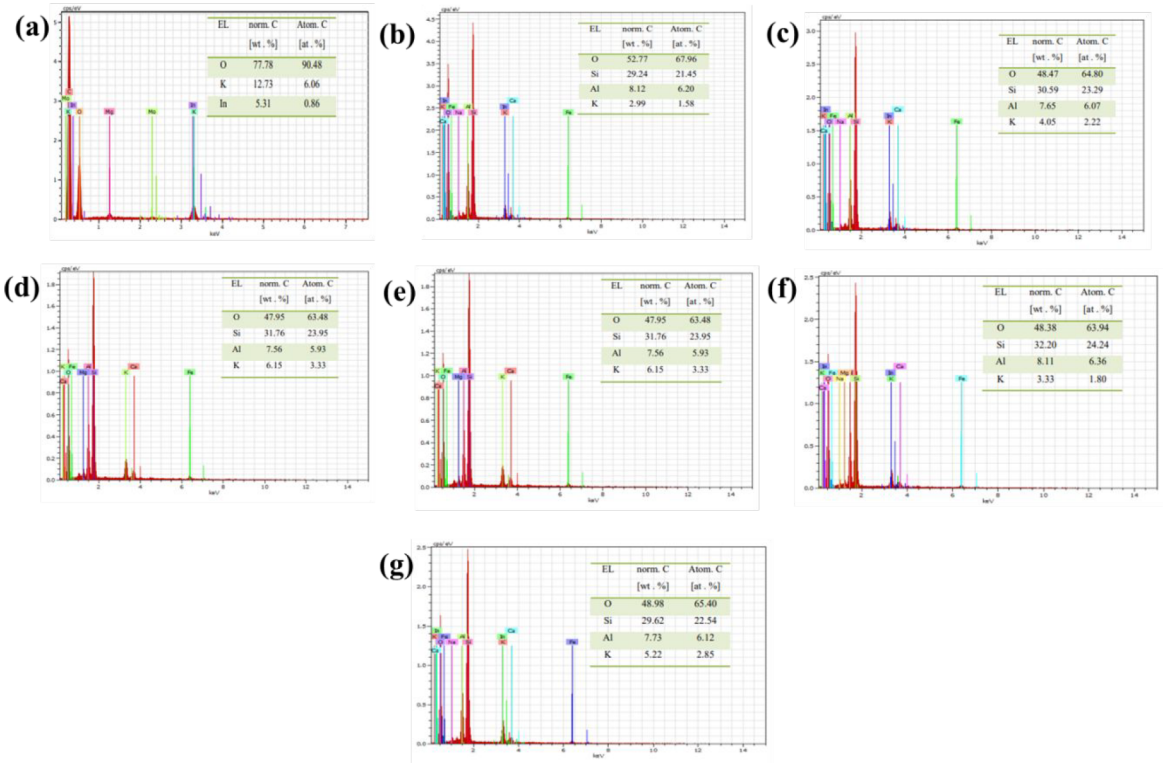

Figure 7. EDX elemental analysis of the sample: (a) (0:100)%; (b) (100:0)%; (c) 95:5)%; (d) (90:10)%; (e) (85:15)%; (f) (80:20)%; and (g) (75:25)%.

of the five samples had not been mixed evenly. This can be seen from the pore diameters on the surface of the tested nanofilters. The results of the pore diameters for all composition variations are as follows: (0:100)% (pure activated charcoal) with average d = 1.676 μm, (100:0)% (pure zeolite) average d = 1.070 μm (95:5)% average d = 2,547 μm, (90:10)% average d = 1.483 μm, (85:15)% average d = 1.548 μm, (80:20)% average d = 2.107 μm, and (75:25)% average d = 1.430 μm. Based on the scanning of the five nanofilters composition variations, it can be seen that the addition of cocoa shell activated charcoal filler in zeolite was able to increase the pore diameter compared to pure zeolite composition, which only had an average value of d = 1.070 μm.

3.6. EDX Analysis. Tests with EDX were carried out to determine the elemental content in the nanofilter that affects the adsorption power of the nanofilter, which can be seen in Figure 7.

Figure 7 shows the elemental content of all sample variations which were activated at 700 °C. The results of the analysis showed that most of the samples contained oxygen, silica, aluminum, ferron, potassium, calcium, charcoal, sodium, indium, and magnesium. The EDX analysis also confirmed that the presence of oxygen elements came from oxygen bound in SiO_2 compounds and free oxygen which was trapped in the nanofilter pores. The presence of oxygen is known to affect the formation of pores on the surface of the nanofilter considering the ability of oxygen to produce uniform small holes which in the end also determines the adsorption ability of the nanofilter. Based on the elemental content, the Si/Al ratio can be calculated, which will also affect the adsorption rate of the sample. The results of the Si/Al ratio of the six samples, (0:100)%, (100:0)%, (95:5)%, (90:10)%, (85:15)%, and (80:20)% were 3.60, 3.99, 4.20, 3.93, 3.97, and 3.83, respectively. From the results obtained, the ratio of the six samples is in the range of 2−5. Thus, all samples are classified as intermediate adsorbers with the type of modernite zeolite.

3.7. X-ray Diffraction (XRD) Analysis. The nanofilters was exposed to an X-ray Diffraction (XRD) analysis to determine the presence of crystalline and amorphous regions in its structure. Figure 8 depicts the nanofilters diffractogram of all composition variations at 700 °C activation temperature.

In samples with a composition of (100:0)%, which can be referred to as pure zeolite matrix, the resulting diffraction

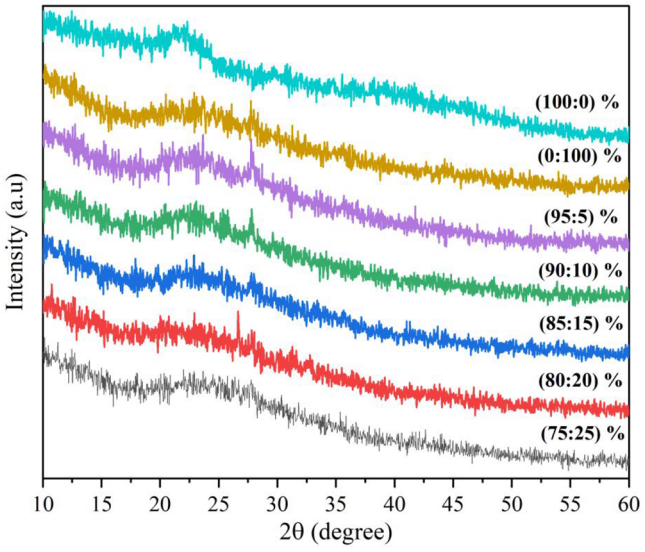

Figure 8. Diffractograms of the nanofilters with an activated temperature of 700 °C.

https://doi.org/10.1021/acsomega.2c03614
ACS Omega 2022, 7, 38417−38425

pattern is amorphous. Furthermore, with the presence of cocoa shell activated charcoal filler, it is expected that there will be an increase in the crystalline intensity of the nanofilter. However, the ensuing diffraction pattern in Figure 8 does not demonstrate a significant difference. All samples had an amorphous shape with nonsharp peaks. This demonstrates that adding cocoa shell activated charcoal to the nanofilter does not increase the crystalline intensity. The degree of crystallinity in the (95:5)% composition nanofilter is 8.41%, with the crystal area fraction of 635.75 and the amorphous area fraction of 7554.67. As a result, the nanofilter with a (95:5)% composition can be mentioned as an amorphous rather than a crystalline compound.

3.8. Fourier Transform Infrared Spectroscopy (FTIR) Analysis. FTIR analysis is intended to determine the functional groups and wave numbers based on the resulting absorption peaks. Figure 9 shows the results of the FTIR nanofilter test for all composition variations which were activated at a temperature of 700 °C.

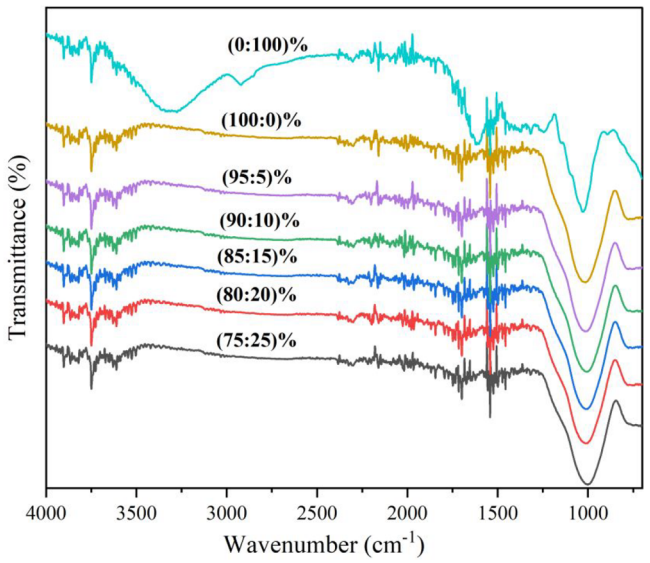

Figure 9. FTIR results of all samples with an activation temperature of 700 °C.

In Figure 9, it can be seen that all observed nanofilter samples showed OH bond peaks for the samples (0:100)%, (100:0)%, (95:5)%, (90:10)%, (85:15)%, (80:20)%, and (75:25)% at wavelengths 3287.36, 3742.43, 3742.79, 3742.35, 3742.53, 3742.57, and 3742.43 cm^{-1} respectively. Furthermore, it was discovered from the graph that all of the samples have the TO_4 [SiO_4] bond peak, which is at 1000–1100 cm^{-1}, as shown in Table 1.

3.9. XRF Analysis. XRF analysis is intended to determine the composition of the elemental compounds contained in the zeolite material used, as shown in Table 2.

The presence of elements in the form of oxides, namely alumina (Al_2O_3) and silica (SiO_2), which are the main components of the framework of natural zeolite and are equal to 10.84% (wt) for alumina and 66.733% (wt) for silica, can be proven based on the XRF test results on the zeolite sample as shown above. As a result, this natural zeolite has a Si/Al ratio of 6.15, indicating that the density of Al atoms in the zeolite crystal framework structure is quite high. This natural zeolite has an alumina (Al_2O_3) purity of 10.882% (wt) and a silica (SiO_2) purity of 67.061% (wt).

Table 1. FTIR Test Results for the TO_4 [SiO_4] Wavelength Bond

No.	Treatment Variations	TO_4 [SiO_4] (cm^{-1})
1	Nanofilter with a (0:100)% composition	1028.95
2	Nanofilter with a (100:0)% composition, activated at temperature of 700 °C	1017.34
3	Nanofilter with a (95:5)% composition, activated at temperature of 700 °C	1013.93
4	Nanofilter with a (90:10) % composition, activated at temperature of 700 °C	1003.27
5	Nanofilter with a (85:15)% composition, activated at temperature of 700 °C	1010.44
6	Nanofilter with a (80:20)% composition, activated at temperature of 700 °C	1012.65
7	Nanofilter with a (75:25)% composition, activated at temperature of 700 °C	1003.09

2.10. Gas Chromatography Analysis on Bioethanol purification. Gas chromatography analysis was carried out to determine the level of purity of bioethanol after being treated with a nanofilter (with a composition of (75:25)% activated at 700 °C), as well as the evaporation process. Table 3 shows the concentration of bioethanol after treatment. Only nanofilters with a composition of (75:25)% with an activation temperature of 700 °C were used in this bioethanol purification test because the samples with this variation had the highest porosity value and the highest water absorption value in the porosity and water adsorption test, respectively.

The optimum concentration of bioethanol was obtained at a contact time of 45 min using a nanofilter ((75:25)% composition which was activated at 700 °C), with the result that the bioethanol concentration increased by about 78.92%. These results support the results of the PSA test and water absorption where the zeolite that has been activated and treated with HEM has a smaller particle size of 118.4 nm and a higher water absorption capacity of 52.08%; thus, it is able to absorb water optimally. This is due to the large number of pores on the surface of the nanofilter. In addition, the contact time of the nanofilter with bioethanol also needs to be considered because it affects the final concentration of bioethanol. The longer the contact time, the more water and bioethanol will be adsorbed on the surface of the nanofilter; this can cause a decrease in the concentration of bioethanol.

CONCLUSION

The activated zeolite produced in this study has a particle size of 118.4 nm and a higher water absorption capacity of 52.08%, which indicates the ability of the zeolite to absorb water. The presence of modernite in the Pahae natural zeolite was validated by the Si/Al ratio from the EDX study, and the amorphous nature of the diffraction pattern nanofilter sample was confirmed by the XRD analysis. The hardness values of the activated samples show that the sample which was activated at temperatures of 700 °C was the sample that has the optimum hardness value. During bioethanol purification, a cocoa shell activated charcoal–zeolite nanofilter was able to absorb water in bioethanol products. The zeolite-activated charcoal nanofilters containing cocoa shells were able to increase the concentration of bioethanol up to 78.92% during the adsorption with a 45 min contact time for water vapor.

https://doi.org/10.1021/acsomega.2c03614
ACS Omega 2022, 7, 38417–38425

Table 2. XRF Test Results Data for Zeolite Samples

Element			Geology			Oxide		
Compd	Conc	Unit	Compd	Conc	Unit	Compd	Conc	Unit
Na	0	%	Na_2O	0	%	Na_2O	0	%
Mg	0.24	%	MgO	0.284	%	MgO	0.283	%
Al	8.742	%	Al_2O_3	10.882	%	Al_2O_3	10.84	%
Si	54.337	%	SiO_2	67.061	%	SiO_2	66.733	%
P	2.961	%	P_2O_5	3.302	%	P_2O_5	3.281	%
Cl	0.024	%	Cl	0.011	%	K_2O	7.908	%
K	14.446	%	K_2O	7.963	%	CaO	5.231	%
Ca	8.969	%	CaO	5.271	%	TiO_2	1.082	%
Ti	1.634	%	Ti	0.654	%	V_2O_5	0.023	%
V	0.034	%	V	0.013	%	Cr_2O_3	0.003	%
Cr	0.006	%	Cr	0.002	%	MnO	0.046	%
Mn	0.093	%	Mn	0.036	%	Fe_2O_3	3.951	%
Fe	7.208	%	Fe_2O_3	3.983	%	ZnO	0.011	%
Zn	0.025	%	Zn	0.009	%	Ga_2O_3	0.005	%

Table 3. Bioethanol Concentration after Treatment with a Nanofilter with a Composition of (75:25)% and Activated at 700 °C

No.	Composition	Contact Time (min)	Initial Bioethanol Concentration (%)	Final Bioethanol Concentration (%)	Increase of Bioethanol Concentration (%)
1	(75:25)%	30	40	47.21	18.02
2		45	40	71.57	78.92
3		60	40	57.62	44.05
4		75	40	51.63	29.07
5		90	40	49.21	23.02

AUTHOR INFORMATION

Corresponding Author

Susilawati − *Department of Physics, Faculty of Mathematics and Natural Sciences, Universitas Sumatera Utara, Medan 20155, Indonesia;* orcid.org/0000-0003-2122-0128; Email: susilawati@usu.ac.id

Authors

Yuan Alfinsyah Sihombing − *Department of Physics, Faculty of Mathematics and Natural Sciences, Universitas Sumatera Utara, Medan 20155, Indonesia*

Siti Utari Rahayu − *Department of Physics, Faculty of Mathematics and Natural Sciences, Universitas Sumatera Utara, Medan 20155, Indonesia*

Lilik Waldiansyah − *Department of Physics, Faculty of Mathematics and Natural Sciences, Universitas Sumatera Utara, Medan 20155, Indonesia*

Yuni Yati Br Sembiring − *Department of Physics, Faculty of Mathematics and Natural Sciences, Universitas Sumatera Utara, Medan 20155, Indonesia*

Complete contact information is available at: https://pubs.acs.org/10.1021/acsomega.2c03614

Notes

The authors declare no competing financial interest.

ACKNOWLEDGMENTS

The author wishes to thank Universitas Sumatera Utara for completely funding this research through the TALENTA 2021 research program on June 16, 2021, under contract no. 6789/UN5.1.R/PPM/2021.

REFERENCES

(1) Owusu, P. A.; Asumadu-Sarkodie, S. A review of renewable energy sources, sustainability issues and climate change mitigation. *Cogent Eng.* **2016**, *3* (1), 1167990.

(2) Zou, C.; Zhao, Q.; Zhang, G.; Xiong, B. Energy revolution: From a fossil energy era to a new energy era. *Nat. Gas Ind. B* **2016**, *3*, 1−11.

(3) Koçar, G.; Civaş, N. An overview of biofuels from energy crops: Current status and future prospects. *Renew Sustain Energy Rev.* **2013**, *28*, 900−916.

(4) Rosales-Calderon, O.; Arantes, V. A Review on Commercial-Scale High-Value Products That Can Be Produced alongside Cellulosic Ethanol. *BioMed. Central.* **2019**, *12*, 240.

(5) Tse, T. J.; Wiens, D. J.; Reaney, M. J. T. Production of bioethanol—a review of factors affecting ethanol yield. *Fermentation.* **2021**, *7*, 268.

(6) Mohd Azhar, S. H.; Abdulla, R.; Jambo, S. A.; Marbawi, H.; Gansaua, J. A.; Faik, A.A. M.; Rodrigues, K. F. Yeasts in sustainable bioethanol production: A review. *Biochem Biophys Reports* **2017**, *10*, 52−61.

(7) Karimi, S.; Yaraki, M. T.; Karri, R. R. A comprehensive review of the adsorption mechanisms and factors influencing the adsorption process from the perspective of bioethanol dehydration. *Renew Sustain Energy Rev.* **2019**, *107*, 535−553.

(8) Al-Asheh, S.; Banat, F.; Al-Lagtah, N. Separation of ethanol−water mixtures using molecular sieves and biobased adsorbents. *Chem. Eng. Res. Des.* **2004**, *82*, 855−864.

(9) Wang, S.; Peng, Y. Natural zeolites as effective adsorbents in water and wastewater treatment. *Chem. Eng. J.* **2010**, *156*, 11−24.

(10) Sudibandriyo, M.; Putri, F. A. The Effect of Various Zeolites as an Adsorbent for Bioethanol Purification using a Fixed Bed Adsorption Column. *Int. J. Technol.* **2020**, *11*, 1300−1308.

(11) Khaleque, A.; Alam, M. M.; Hoque, M.; Mondal, S.; Haider, J. B.; Xu, B.; Johir, M. A. H.; Karmakar, A. K.; Zhou, J. L.; Ahmed, M. B.; Moni, M. A. Zeolite synthesis from low-cost materials and environmental applications: A review. *Environ. Adv.* **2020**, *2*, 100019.

(12) Calabrese, L. Anticorrosion behavior of zeolite coatings obtained by in situ crystallization: A critical review. *Materials (Basel)* **2019**, *12* (1), 12010059.
(13) Zarrintaj, P.; Mahmodi, G.; Manouchehri, S. Zeolite in tissue engineering: Opportunities and challenges. *MedComm.* **2020**, *1*, 5−34.
(14) Kusumaningtyas, M. P.; Regina, G. L. D.; Ade, L. N. F.; Haiyina, H. A.; Nura, H. H.; Darminto, D. Synthesis of zeolites from Lombok pumice as silica source for ion exchanger. *1st Int. Basic Sci. Conf Towar Ext use basic Sci. enhancing Heal Environ. energy Biotechnol* **2017**, 244−247.
(15) Li, Y.; Li, L.; Yu, J. Applications of Zeolites in Sustainable Chemistry. *Chem.* **2017**, *3*, 928−949.
(16) Nasution, T. I.; Susilawati; Zebua, F.; Nainggolan, H.; Nainggolan, I. Manufacture of Water Vapour Filter Based on Natural Pahae Zeolite Used for Hydrogen Fueled Motor Cycle. *Appl. Mech Mater.* **2015**, *754*−*755*, 789−793.
(17) Susilawati; Nasution, T. I.; Zebua, F.; Nainggolan, H. Hydrogen purification using natural pahae zeolit and cocoa rind based filter. *Int. J. Appl. Eng. Res.* **2017**, *12*, 3914−3918.
(18) Susilawati; Nasruddin, M. N.; Kurniawan, C.; Nainggolan, I.; Sihombing, Y. A. Ethanol Purification Using Active Natural Pahae Zeolite by Adsorption Distillation Method. *J. Phys. Conf Ser.* **2018**, *1116*, 032037.
(19) Heraldy, E.; SW, H.; Sulistiyono, S. Characterization and Activation of Natural Zeolit From Ponorogo. *Indones J. Chem.* **2003**, *3*, 91−97.
(20) Sulistyowati, N.; Sriyanti, S.; Darmawan, A. Effect of Acid on Natural Zeolite Dealumination on Indigo Carmine Adsorption Capability. *J. Kim Sains dan Apl.* **2018**, *21*, 102−106.
(21) Fuss, V. L. B.; Bruj, G.; Dordai, L.; Roman, M.; Cadar, O.; Becze, A. Evaluation of the impact of different natural zeolite treatments on the capacity of eliminating/reducing odors and toxic compounds. *Materials (Basel).* **2021**, *14*. No. .3724
(22) Susilawati; Nasruddin, M. N.; Sihombing, Y. A.; Pakpahan, S. N. Y.; Ferdiansyah, B. Preparation of pahae natural zeolite nanoparticles using high energy milling and its potential for bioethanol purification. *Rasayan J. Chem.* **2021**, *14*, 1265−1272.
(23) Ackley, M. W.; Rege, S. U.; Saxena, H. Application of natural zeolites in the purification and separation of gases. *Microporous Mesoporous Mater.* **2003**, *61*, 25−42.
(24) Tsai, W. T.; Lai, C. W.; Hsien, K. J. Effect of particle size of activated clay on the adsorption of paraquat from aqueous solution. *J. Colloid Interface Sci.* **2003**, *263*, 29−34.
(25) Adam, M. R.; Othman, M. H. D.; Kadir, S. H. S. A. Influence of the natural zeolite particle size toward the ammonia adsorption activity in ceramic hollow fiber membrane. *Membranes (Basel)* **2020**, *10*, 1−18.
(26) Naji, S. Z.; Tye, C. T. A review of the synthesis of activated carbon for biodiesel production: Precursor, preparation, and modification. *Energy Convers Manag X.* **2022**, *13*, 100152.
(27) Olchowski, R.; Zieba, E.; Giannakoudakis, D. A.; Anastopoulos, I.; Dobrowolski, R.; Barczak, M. Tailoring surface chemistry of sugar-derived ordered mesoporous carbons towards efficient removal of diclofenac from aquatic environments. *Materials (Basel)* **2020**, *13*, 1−17.
(28) Şahin, Ö.; Saka, C. Preparation and characterization of activated carbon from acorn shell by physical activation with H2O-CO2 in two-step pretreatment. *Bioresour. Technol.* **2013**, *136*, 163−168.
(29) Goh, P. S.; Wong, K. C.; Ismail, A. F. Nanocomposite membranes for liquid and gas separations from the perspective of nanostructure dimensions. *Membranes (Basel)* **2020**, *10*, 1−29.
(30) Le, N. L.; Nunes, S. P. Materials and membrane technologies for water and energy sustainability. *Sustain Mater. Technol.* **2016**, *7*, 1−28.
(31) Ouattara, L. Y.; Kouassi, E. K. A.; Soro, D. Cocoa Pod Husks as Potential Sources of Renewable High-Value-Added Products: A Review of Current Valorizations and Future Prospects. *Bioresources* **2021**, 1988−2020.
(32) Susilawati; Sani, A.; Sihombing, Y. A.; Pakpahan, S. N. Y.; Ferdiansyah, B. The utilization of cocoa rind waste and clay as filter materials in purifying well water. *AIP Conf Proc.* **2020**, *2221*, 0−9.
(33) Susilawati; Siburian, J.; Sihombing, Y. A.; Ferdiansyah, B.; Pakpahan, S. N. Y. Fabrication and characterization of physical and mechanical properties based on clay and cacao rind porous ceramics. *AIP Conf Proc.* **2020**, *2221*, 0−9.
(34) ASTM C20-00. Standard Test Methods for Apparent Porosity, Water Absorption, Apparent Specific Gravity, and Bulk Density of Burned Refractory Brick and Shapes by Boiling Water. *Am. Soc. Test Mater.* **2015**, *00*, 1−3.
(35) ASTMC642-06. Standar Test Method Density, Absorption, Voids Hardened Concr. *Am. Soc. Test Mater.* **2008**, 11−13.
(36) Masturi, M.; Cristina, A.; Istiana, N.; Sunarno, S.; Dwijananti, P. Ethanol Production from Fermentation of Arum Manis Mango Seeds (*Mangifera indica* L.) using *Saccharomyces Crevisiaea*. *J. Bahan Alam Terbarukan* **2017**, *6*, 56−60.
(37) Bušić, A.; Mardetko, N.; Kundas, S. Bioethanol production from renewable raw materials and its separation and purification: A review. *Food Technol. Biotechnol* **2018**, *56*, 289−311.
(38) Siswanto, Y. A.; Hariyanto, M. Synthesis of Zinc Oxide (ZnO) Nanoparticle By Mechano-Chemical Method. *Proceeding The 1st IBSC: Towards The Extended Use Of Basic Science For Enhancing Health, Environment, Energy And Biotechnology* **2017**, *1*, 174−176.
(39) Naghdi, M.; Taheran, M.; Brar, S. K. A green method for production of nanobiochar by ball milling- optimization and characterization. *J. Clean Prod.* **2017**, *164*, 1394−1405.
(40) Tadda, M.; Ahsan, A.; Shitu, A. A Review on Activated Carbon from Biowaste: Process, Application and Prospects. *J. Adv. Civ. Eng. Pract. Res.* **2018**, *5*, 82−83.
(41) Burris, L. E.; Juenger, M. C. G. Effect of calcination on the reactivity of natural clinoptilolite zeolites used as supplementary cementitious materials. *Constr Build Mater.* **2020**, *258*, 119988.
(42) Pallarés, J.; González-Cencerrado, A.; Arauzo, I. Production and characterization of activated carbon from barley straw by physical activation with carbon dioxide and steam. *Biomass and Bioenergy.* **2018**, *115*, 64−73.
(43) Byamba-Ochir, N.; Shim, W. G.; Balathanigaimani, M. S.; Moon, H. Highly porous activated carbons prepared from carbon rich Mongolian anthracite by direct NaOH activation. *Appl. Surf. Sci.* **2016**, *379*, 331−337.
(44) Yahya, M. A.; Al-Qodah, Z.; Ngah, C. W. Z. Agricultural bio-waste materials as potential sustainable precursors used for activated carbon production: A review. *Renew Sustain Energy Rev.* **2015**, *46*, 218−235.
(45) Bouchelta, C.; Medjram, M. S.; Bertrand, O.; Bellat, J. P. Preparation and characterization of activated carbon from date stones by physical activation with steam. *J. Anal Appl. Pyrolysis.* **2008**, *82* (1), 70−77.

https://doi.org/10.1021/acsomega.2c03614
ACS Omega 2022, 7, 38417−38425